

MINISTRY OF EDUCATION AND SCIENCE OF THE REPUBLIC OF  
KAZAKHSTAN

Kazakh National Research Technical University named after K.I. Satpayev

Institute of Geology, Oil and Mining

Department of Oil, Gas and Ore Geophysics

Kasymkul Ernur Beybituly

Using the results of dynamic interpretation and attribute analysis of 3D seismic data  
to predict the reservoir properties of productive horizons

**DIPLOMA WORK**

Specialty 5B070600 – «Geology and exploration of mineral deposits»

Almaty 2020

MINISTRY OF EDUCATION AND SCIENCE OF THE REPUBLIC OF  
KAZAKHSTAN

Kazakh National Research Technical University named after K.I. Satpayev

Institute of Geology, Oil and Mining

Department of Oil, Gas and Ore Geophysics

**ADMITTED TO DEFENCE**

Head of the Department of  
Geophysics

Doctor of geol.-miner. sciences,  
professor



Abetov A.E.

“ ”

\_\_\_\_\_ 2020y.

**DIPLOMA WORK**

Topic: “ Using the results of dynamic interpretation and attribute analysis of 3D seismic data to predict the reservoir properties of productive horizons”

Specialty 5B070600 – «Geology and exploration of mineral deposits»

Done by

Kasymkul Ernur Beybituly

Scientific supervisor  
PhD, Associate professor



\_\_\_\_\_ Akhmetzhanov A.Zh.

“ ”

\_\_\_\_\_ 2020y.

Almaty 2020

MINISTRY OF EDUCATION AND SCIENCE OF THE REPUBLIC OF  
KAZAKHSTAN

Kazakh National Research Technical University named after K.I. Satpayev

Institute of Geology, Oil and Mining

Department of Oil, Gas and Ore Geophysics

Specialty 5B070600 – Geology and exploration of mineral deposits

**APPROVED BY**

Head of the Department of  
Geophysics

Doctor of geol.-miner. sciences,  
professor



Abetov A.E.

“ \_\_\_\_\_ ”

2020y.

**THE TASK**

**to complete the diploma work**

Student Kasymkul Ernur Beybituly

Topic: “Using the results of dynamic interpretation and attribute analysis of 3D seismic data to predict the reservoir properties of productive horizons”

Approved by order of the Rector of the University №762–b from "27" January 2020y.

Submission deadline of the completed work " \_\_ " \_\_\_\_\_ 2020y.

Initial data for the diploma work: were selected during the completion of industrial practice

Summary of the diploma work:

a) General information about the area of North Buzachi deposit (geological-geophysical study, tectonics, stratigraphy, presence of oil and gas)

b) Analysis of geological and geophysical data in the area of deposit

c) Processing of seismic materials

d) Interpretation of geological and geophysical materials

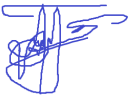
The list of graphic material: are presented \_\_\_\_ slides of presentation work

Recommended main literature: «Tectonics of the pre-Jurassic sedimentary complex of the west of the Turan Plate», «The deep structure and mineral resources of Kazakhstan».

**GRAPH**  
of the diploma work preparation

Section Names, list of issues under development	Submission deadline to scientific supervisor	Notes
Geological-geophysical study. Presence of oil and gas		
Analysis of geological and geophysical data in the area of deposit		
Processing of seismic materials		
Interpretation of geological and geophysical materials		

**Signatures**  
of the consultants and standard controller for the completed diploma work with an indication of the sections of work related to them

Section Names	Consultants, name, patronymic, surname (academic degree, title)	Date of signing	Signature
Geological-geophysical study. Presence of oil and gas			
Analysis of geological and geophysical data in the area of deposit			
Processing and interpretation of geological and geophysical materials			
Standard controller	M.M.Aliakbar Tutor		

Scientific supervisor



Akhmetzhanov A.Zh.

*signature*

The student fulfilling the task



Kasymkul E.B

*signature*

Date

" \_ " "

\_\_\_\_\_2020y.

## **ABSTRACT**

To the diploma work «Using the results of dynamic interpretation and attribute analysis of 3D seismic data to predict the reservoir properties of productive horizons»

The work consists of introduction, 4 chapters, conclusion, list of references and applications.

This brief work is intended to review the results of 3D seismic surveys conducted at the Buzachi field.

The North Buzachi field is located on the Buzachi Peninsula, on the northeastern shore of the Caspian Sea. This work was done to create a seismic-geological model of the North Buzachi field, which contains detailed operational details during the Neocomian and Jurassic periods.

The introduction examines the relevance of the study and provides an overview of the work done on this topic. The goals, objectives and research methods are established. The general section contains a general description of the workspace. Summarized data on the geological and geophysical studies of the region are presented. A brief geological description of the Severo-Buzachinsky field is given, containing information on stratigraphy, tectonics, oil and gas.

Using the example of the North Buzachi deposit, was developed a methodology for separating the Neocomian and Jurassic sediments using the methods of dynamic interpretation and seismic inversion.

During the stages of processing and interpretation, was used the software of the "Paradigm" company.

The last section provides conclusions on the results of the work, the advantages of a three-dimensional study of dynamic interpretation in terms of the obtained geological results.

## АННОТАЦИЯ

К дипломной работе «Использование результатов динамической интерпретации и атрибутивного анализа сейсмических данных 3D для прогноза фильтрационно-емкостных свойств продуктивных горизонтов»

Работа состоит из введения, 4 глав, заключения, списка использованных источников и приложений.

Эта краткая работа предназначена для обзора результатов 3D сейсмических исследований, проведенных на месторождении Бузачи.

Месторождение Северная Бузачи расположено на полуострове Бузачи, на северо-восточном берегу Каспийского моря. Эта работа была выполнена для создания сейсмико-геологической модели месторождения Северные Бузачи, в котором имеются подробные эксплуатационные детали в периоды неокома и юры.

На примере месторождения Северные Бузачи были отработана методика расчленения неокома и юрских залежей с использованием методов динамической интерпретации и сейсмической инверсии.

При обработке и интерпретации использовалось программное обеспечение компании "Paradigm".

Во введении рассматривается актуальность исследования и дается обзор работы, проделанной по этой теме. Цели, задачи и методы исследования установлены. Общий раздел содержит общее описание рабочей области. Приведены обобщенные данные о геолого-геофизических исследованиях района. Дано краткое геологическое описание Северо-Бузачинского месторождения, содержащее информацию о стратиграфии, тектонике, нефти и газе. Проведен анализ работы прошлых лет. Главы 3 и 4 посвящены результатам обработки и интерпретации сейсмических данных соответственно.

В последнем разделе приводятся выводы по результатам работы, преимуществам трехмерного исследования динамической интерпретации с точки зрения полученных геологических результатов.

## АНДАТПА

Дипломдық жұмысқа «Динамикалық интерпретация және 3D сейсмикалық деректердің атрибуттық талдау нәтижелерін өнімді горизонттардың коллекторлық қасиеттерін болжау үшін пайдалану»

Дипломдық жұмыс кіріспеден, 4 тараудан, қорытындыдан, пайдаланылған әдебиеттер тізімінен және қосымшалардан тұрады.

Бұл жұмыс Бозашы кен орнында жүргізілген 3D сейсмосбарлау нәтижелерін саралауға арналған. Солтүстік Бозашы кен орны Бозашы түбегінде, Каспий теңізінің солтүстік-шығыс жағалауында орналасқан.

Бұл жұмыс Солтүстік Бозашы кен орнының сейсмикалық-геологиялық моделін құру үшін орындалды, неокомиялық және юра кезеңдерінде егжей-тегжейлі өндіріс бөліктері бар.

Солтүстік Бозашы кен орны мысалын қолдана отырып, динамикалық интерпретация және сейсмикалық инверсия әдістерін қолдана отырып, неокома және юра шөгінділерін бөлу әдістемесі жасалды.

Өңдеу және интерпретация кезінде "Paradigm" компаниясының бағдарламалық жасақтамасы қолданылды.

Кіріспеде зерттеудің өзектілігі қарастырылып, белгіленген тақырыпта орындалған жұмыстарға шолу жүргізілген. Зерттеудің мақсаттары, міндеттері мен әдістері қойылған. Жалпы бөлімде жұмыс ауданы туралы жалпы сипаттамасы беріледі. Ауданның геологиялық-геофизикалық зерттелуі туралы жалпыланған мәліметтер келтіріледі. Стратиграфия, тектоника, мұнай-газдылығы туралы мәліметтерді ұсына отырып, Солтүстік Бозашы кен орнының қысқаша геологиялық сипаттамасы беріледі. Өткен жылдардағы жұмыстарды талдау жүргізіледі. 3 және 4-тараулар тиісінше өңдеу жұмыстарына және сейсмикалық мәліметтерді интерпретациялау нәтижелеріне арналған.

Қорытынды бөлімінде жұмыс нәтижелері бойынша қорытындылар берілген, алынған геологиялық нәтижелер жағынан динамикалық интерпретацияның 3D барлау артықшылықтары көрсетілген.

# CONTENTS

Introduction	9
1 General information on the area of work	10
2 Geological and geophysical characteristics of the field.	11
2.1 Geophysical knowledge	11
2.2 Brief geological and tectonic characteristics of the area	12
2.3. Stratigraphy	12
2.4 Tectonics	16
2.5 Presence of oil and gas	17
3 Field seismic data processing	21
3.1 Processing of seismic data in the time domain	21
3.2 Interpretation processing	22
3.2.1 Migration before summation in the time domain	22
3.2.2 Migration before summation in the deep region	22
3.2.3 Construction of the deep-speed model (DSM)	23
3.2.4 Migration Aperture Testing	23
3.2.5 Migration procedure and summation	23
3.2.6 Post migration procedure	23
4 Interpretation of seismic materials	25
4.1 Database for interpretation	25
4.2 Stratification of reflecting horizons	27
4.3 Dynamic interpretation and attribute analysis.	27
4.3.1 Analysis of petrophysical properties of rocks for the problems of AVO analysis and amplitude inversion	27
4.3.2 Studying the stiffness properties of the target interval.	28
4.4 Attribute and seismic facies analysis	28
4.5 Characterization of reservoirs.	29
Conclusion	31
List of references	32
Appendix A	34
Appendix B	35
Appendix C	36
Appendix D	37
Appendix E	39
Appendix F	40

## INTRODUCTION

This graduation work done on the topic «Using the results of the dynamic Interpretation and the attribute analysis of 3D seismic data to predict the reservoir properties of Productive Horizons»

The purpose of these works is to build a seismic-geological model of the North Buzachi field throughout the section with detailed production parts in the Neocomian and Jurassic.

Recoverable reserves are estimated at approximately 50-80 million tons of oil, geological reserves - at 218 million tons of oil. To extract and search for potential oil reserves, advanced types of work, processing and interpretation are used. Building a 3D geological model of the field is an integral part of the seismic interpretation.

In preparing the field for commercial operation, it is necessary to build a conceptual model that reflects the internal structure of the studied objects. Conceptual modeling, in turn, is based on the synergy of analysis and interpretation of all the geological, geophysical and seismic information available in the study area using various types of attribute analysis, which allows predicting changes in lithology and filtration-reservoir properties of rocks, as well as evaluating the reserves of the deposit. The conceptual geological model summarizes the sedimentation, petrophysical and seismic facies models, combining them in the 3D geological model of the field.

This paper describes the geological structure of the area, tectonics and stratigraphy of the North Buzachi field. In this diploma are showed data about works which were done in this territory, data on processing and interpretation. A special place in the diploma is given to the consideration of dynamic interpretation and attribute analysis

## **1 General information about the area of work**

The Buzachi Peninsula is one of the most important oil producing regions of Western Kazakhstan. The North Buzachi field is located on the Buzachi Peninsula within the northeastern coastal part of the Caspian Sea (Figure A1).

Using the example of the Saigak deposit, the author tried to analyze the effectiveness of processing methods and interpretation of seismic data on Permian-Triassic sediments using dynamic interpretation and seismic inversion methods.

The closest settlements are the district center of the Mangistau region, the village of Shetpe (120 km from the field to the southeast) and the regional center of the Mangystau region, the city of Aktau (260 km south of the field).

Orographically, the area is a mildly hilly plain. The relief of the 3D shooting area varies between -28 and -22 meters (Figure A2).

The climate of the region is sharply continental with seasonal temperature fluctuations from +30 + 45°C in the summer to -30°C in the winter, the average annual air temperature + 10.4 ° C. Precipitation is insignificant and mainly falls on the autumn-winter period.

A high-voltage transmission line LEP-110 passes through the North Buzachi field, providing it with electricity.

The nearest Aktau-Kalamkas motorway is 8 km from the working village. The Kalamkas-Karazhanbas-Atyrau-Samara oil pipeline and the Kalamkas-Karazhanbas gas pipeline were laid near the freeway. There is no hydrographic network. The presence of numerous litters, representing drainage depressions, which are filled with atmospheric precipitation in the autumn and winter, is impassable for vehicles. The Kiyakty-Karazhanbas-Kalamkas seawater supply system, the Volga-Kalamkas Volga water supply system and the Kiyakty-Karazhanbas-Kalamkas drinking water supply system.

In the area of the deposit there are relatively shallow, low-depleted wells with potable low-saline water that were used during exploration. In addition, drinking water for oil scouts was delivered by tankers from the village. Tuschikuduk, located 120 km, and underground water of the Upper Albian horizons, as well as sea water, were used for technical water supply. Currently, tap water is used.

Since the deposit occupies the central part of the Bolshoi Litter tract and is represented by sorrow and crust-puffy salt marshes, more than 70% of the territory is completely devoid of vegetation, and in the rest of the area it is extremely poor and is represented by species typical of semi-deserts.

## **2 Geological and geophysical characteristics of the field**

### **2.1 Geophysical knowledge**

The North Buzachi deposits within the eastern side of the Caspian Basin have been studied by an expanded set of geological and geophysical methods. The results of these studies are discussed in detail in the relevant production and thematic reports.

Information on the geological structure of the area of work was obtained from drilling deep wells and geophysical, mainly seismic exploration.

Structural exploration and exploratory drilling at the field was carried out in the period from 1975 to 1977, production drilling began in 1999 and is currently ongoing.

Work on the integration of 3 D seismic exploration and drilling in the reporting area has been carried out for the past 9 years. First, Texaco carried out an interpretation of the central cube in 2001 using new wells that had been drilled by then (about 50 NB series wells and G and K series wells). The western and eastern parts of the license area were covered only with 2 D profiles . This was the first, but nonetheless successful attempt to create a modern model of the field structure using dynamic interpretation of the productive part of the section. The results of this work made it possible to evaluate the effectiveness of 3 D seismic exploration.

The second attempt to further study the licensed area was made after completing 3 D seismic exploration in the eastern part of the field. The work was carried out taking into account the increased to 350 number of wells in 2007. The main problem that could not be fully resolved was the creation of a common cube in the central and eastern parts of the field. This was primarily due to an attempt to combine cubes at the level of existing cubes processing options. Experience has shown that this was an erroneous decision. The second very important problem for the work of this period was the desire to minimize the time frame for linking well information and seismic exploration. This also negatively affected the overall, fairly good results of the second stage. The most important achievement of this stage is the experience that made it possible to understand what should be done if there are several different surveys and a large number of drilled wells.

It was the experience of the years 2007-2008 that made it possible to understand that in order to successfully solve the problem of creating a modern version of the seismic-geological model of the structure of the North Buzachi field, the following conditions must be met:

- combining all surveys at the level of the initial seismograms and performing migration along the combined cube;
- depth migration and work with a deep cube for structural-kinematic interpretation and with temporary cubes for dynamic interpretation and attribute analysis;

- implementation of the GIS interpretation and the creation of a model of sandstone formations within the framework of a single project across the entire licensed area.

The execution of work on this report, in essence, is the implementation of such an approach.

## **2.2 Brief geological and tectonic characteristics of the area**

The litho-stratigraphic characterization of sediments is given on the basis of a generalization of the results of seismic studies, lithological-petrographic analyzes, logging data and a description of the sludge in this area.

Upper Paleozoic, Early Triassic, Middle Jurassic and Early Cretaceous deposits were discovered by drilling at the North Buzachi field.

When stratigraphically dissecting the section of the field and describing its lithological and facies characteristics, the GIS materials of all drilled exploratory, exploratory and production wells were used, as well as the results of lithological-petrographic and biostratigraphic core studies.

## **2.3 Stratigraphy**

Core material most fully characterized deposits of the Middle Jurassic, Neocomian and Aptian, to a lesser extent - the Triassic.

### **Upper Paleozoic ( Pz 2 )**

Upper Paleozoic sediments were discovered only in parametric well No. 7 (interval 1987–3500 m), drilled outside the area of the present studies. The entire thickness of the Upper Paleozoic is composed (according to V.N. Krivonos) of unevenly interlaced dark-colored strongly carbonate mudstones and marl-like organogenic clastic limestones. Among these rocks, light gray organogenic clastic and breccia dolomite limestones are noted. The main component of organogenic clastic limestones are rounded fragments of carbonate rocks, thin and small in marl-like limestones, medium and large in light gray limestone differences. In the latter, along with this, there is also a significant number of fragments of shells of large foraminifera (fusulinids, etc.), brachiopods, and less commonly, ostracods. In addition, there is a significant amount of residues of segments of crinoids, calcareous algae, corals, calcified radiolarians. Less frequently, fauna fragments are noted in marl-like finely clastic limestones.

Light gray limestone differences are characterized by numerous meandering and branching cracks that cut these rocks in different directions. Most often, cracks are filled with calcite veins or clay-carbonaceous matter. Separate cracks, as well as

pores in recrystallized and completely dolomitic areas of limestone, are sometimes made of light brown and brown bitumen of the oil series.

According to K. Beisenova, limestones of this sequence in the intervals of 2172–2177 m and 2430–2435 m contain a very poor foraminifera complex, which does not allow dating their deposits more accurately than stone-lower Permian ones. N.K. Gordeev, on the basis of the same complex of foraminifera, determines the age of sediments as Middle Carboniferous-Early Permian.

### **Triassic system (T)**

Triassic deposits within the considered area were discovered by a significant number of wells and are represented only by the lower section.

They are composed of argillite-like clays and mudstones of brown-brown, less often greenish-gray color, and fine-grained sandstones with subordinate interlayers of limestone, marl and siltstone. Among the organic residues identified core exploration wells defined ostracods *Gerdalia Vetlugensis* Bel., *G. Clara* Mich., *The G. Defecta* Schl., *Darwinula* sp., Miospores *Punctatisporites* sp., *Verrucosisporites* sp., *Cycloverrutriletes presselensis* Schulz, *Platysaccus* sp., *Cucloverrutriletes triassicus* Maid, *Florinites* sp., Microphytoplankton. Based on these definitions, the age of the sediments dates back to the Early Triassic (Indo-Olenek).

The results of biostratigraphic core studies indicate a continental - fluviodeltoe sedimentation medium.

The maximum discovered thickness of the Triassic deposits is 2686 m (well G3, drilled outside the study area). In other wells, it ranges from the first units to 69 m (well G146).

### **Jurassic System (J)**

Jurassic deposits were discovered in whole or in part by the majority of structural exploration, exploration and production wells. They lie sharply disagreeably on the blurry and weathered surface of the Triassic formations. On the whole, the Jurassic sediments are lithologically represented by interbedded gray-colored clays, siltstones, and sandstones.

According to the results of analysis of the spore-pollen complexes, as well as on the basis of a few finds of pelecipods, Jurassic sediments are represented only by the middle section in the volume of the Bajo and Bati tiers.

#### **Middle Department (J<sub>2</sub>)**

##### **Lower Bajos - (J<sub>2</sub>bj<sub>1</sub>)**

The Lower Bayosian deposits are represented by dark gray sand with a brownish tint, fine-grained, with interlayers of clay, inclusions of coal and charred plant residues. Among the organic residues, myospores *Cytheidites Minor* Coup, *Convrrucosisporites crocinus* Bolch, *Araucaria*

cidites sp ., Pinuspollenites sp ., Neoraisfrikia ef . roduudiformis Tarass , Leptolepidites verrucatus Coup , Classopllis sp ., Tripartina Variabilis Mal ., Piceapollenites sp ., Klukisporites , Cyathidites sp . , freshwater algae and microphytoplankton.

By lithological features and the age of organic residues, these deposits are compared with the Karadirmen suite of the Lower Bios age of the Mountain Mangyshlak.

At the bottom of the section, continental (lake-bog and lagoon-delta) facies are developed, which are replaced by facies of coastal shallow water (desalinated bay, channel, delta, and bar facies) above .

### **Upper Bajos - Baht (J<sub>2</sub> b<sub>2</sub> -J<sub>2</sub> bt )**

Incision composed of sand dark gray with brownish tint, fine-grained, quartz, bituminous, with interbedded clays dark gray, with fragments of gastropods, ostracods, foraminifera and microfossils: Cyathidites sp ., Tripartina variabilis the Mal ., Piceapollenites sp ., Neoraistrika rotundiforma Tarass , Leptolepidites sp ., Pinuspollenites sp ., Densoisporites sp ., Lycopodiumsporites sp ., Classopollis sp ., Os munda j urassica , Klukisporites , Disaceites gen . sp . ), as well as with microphytoplankton.

According to the species composition of microfossils, the host sediments are compared with the Bazarlinskaya suite of Gorny Mangyshlak, whose age, based on palyn complexes and the fauna of bivalves and ammonites, is considered to be Upper Bios-Bati.

The thickness of the Middle Jurassic sediments varies from a few meters in the area of the Triassic sediments under the surface of the pre-Cretaceous erosion to 238 m (well SB15).

### **Cretaceous system (C)**

Cretaceous rocks unconformably lie on the eroded surface of Middle Jurassic, and sometimes Lower Triassic deposits. They are represented by the lower section and include deposits of the Neocomian nadjarus, Aptian and Albian tiers.

#### **Lower section (K<sub>1</sub>)**

##### **Neocomian nadjury ( K<sub>1</sub> nc )**

The lower part of the section, related to the Berrias-Valanginian and lower parts of the Hauterivian stages, is lithologically represented by grayish, fine-grained, slightly cemented sandstones; clay gray, greenish-gray and brick-red, compacted, non-layered, unknown, turning in the upper part into carbonate, silty, micaceous; sands of gray-brown, fine-grained, clayey; siltstones weakly cemented. Rare fragments of greenish-gray microgranular limestones and fragments of charred plant residues are noted. In these deposits, foraminifers are noted : Glomospirella multivoluta , Lagenomina bartensteini Mjatl ., Recurvoides ex gr . princeps , Triplasia sp ., Lenticulina andromeda Esp . et Sig ., L . espitaliei Dieni et Massari and

palynomorphs: *Classopollis* sp ., *Piceapollenites mesozoicus* , *Pinuspollenites divulgatus* , *Cedripites* sp ., *Araucariacidites australis* , *Cycadopites* sp ., *Gleicheniidites senonicus* , *Plicifera delicate* , etc.

The formation of these deposits occurred in shallow marine and slightly deserted basins in a hot and fairly humid climate.

The upper part of the Neocomian section (the upper Hauterivian - Barrem) is represented by the interbedding of red-brown, greenish-gray clays, siltstones of fine-coarse-grained, sandstones of fine-grained, polymictic, siltstone and sands of gray to black, fine-grained, non-carbonate, quartz.

Sandy varieties consist of sandstones with clay cement with well-rounded pebbles and siltstones. By the beginning of the barrem, transgression of the sea occurs with the formation of shallow-water marine formations, mainly clays with rare intercalations of siltstones and sandstones.

The thickness of the Neocomian sub-tier varies from 100 to 179 m (well K-96).

**The Aptian tier ( K<sub>1a</sub> )** with stratigraphic disagreement overlaps the neocomian rocks. At the base of the tier is a basal sand-siltstone horizon up to 20 m thick, composed of coarse-grained gray siltstone and fine-grained sandstone, siltstone, with a small content of gravel and gravel. Above lies a stratum of black non-layered clays with rare interlayers of small marly septarian nodules. Dark gray clays interbedded with siltstones also appear in the upper part of the section. The thickness of the tier varies from 90 to 130 m.

**The Albian tier ( K<sub>1al</sub> )** , represented only by the lower **sub-tier** , lies on the Aptian deposits with a slight erosion, due to which a clear contact between the Apt and the album is well traced on the logs. In lithological terms, the Albian layer is represented mainly by sand-aleuritic rock varieties, interbedded with clay rocks. In the bottom part of the section and in the middle of it, ammonites of the lower and upper biostratigraphic zones of the lower alba, respectively, were found.

The thickness of the tier varies from 180 to 460 m.

Aptian and Albanian sediments formed during marine transgression in a shallow basin.

### **Quaternary deposits ( Q )**

The Quaternary sediments crowning the section of the area, with stratigraphic and angular disagreement, lie on the Lower Cretaceous sediments and are composed of sands, loams and sandy loams deposited in an arid climate. The thickness of the deposits does not exceed 10–12 m.

## 2.4 Tectonics

In recent years, many variations of the tectonic structure of the articulation zone of the Caspian Basin and its southern margin have appeared. After analyzing the proposed schemes, from the position of their maximum correspondence to seismic data (which has been carried out in large volumes in recent years, both in the Caspian Sea and on the Buzachi Peninsula), the authors of this work preferred a point of view on this issue, outlined and illustrated in the work Yu.A. Volozh.

In accordance with this work, it is assumed that the tectonic position of the North Buzachi deposit is such that it is located in the southern part of the Riphean-Cenozoic Caspian basin of the East European platform, in the zone of its articulation with the Mesozoic-Cenozoic Scythian-Turan plate of the Epigerian Eurasian platform (Fig. A2). Moreover, the articulation of these spirits of superordinate structural elements occurs according to a system of regional shifts. In the case under study, this is the western section of the South Emba Shift. With this interpretation of the tectonic position of the area of the Northern Buzachi deposit, it turns out that its northern part is above the pre-Jurassic base formed in the conditions of a passive margin (the Caspian depression), and the southern part is above the system of Triassic grabens thrust over it (the northern marginal zone of the Scythian-Turan plate)

A larger-scale tectonic arrangement of the reporting area is shown in Figure 1.5, from which it follows that it is within the North-Buzachinsky arch.

The Jurassic-Cenozoic platform cover completely covers the buried pre-Jurassic base. For the Severo-Buzachinsky arch, as well as for the Turan plate as a whole, the inherited development of the main tectonic elements of the platform cover from the shape of the pre-Jurassic relief is established.

The formation of the current position of the North-Buzachin structure has left its mark on the activation of tectonic movements in adjacent orogenic areas. These movements led to the active formation of local structures, the revitalization of movements along the faults of the ancient formation (along regional shifts) and the formation of new local discontinuous disturbances in the upper parts of the sedimentary cover

The surface of the foundation, judging by the nature of the reflecting horizon  $P_3$ , has a block structure. In the axial part of the Akzhar-Karatyubinsky uplift and in the Zap. There are two horsts with a throw-up amplitude of up to 400-500m.

The thickness of the subsalt section increases regionally from west to east. Its maximum values are recorded on Tereshkovskaya Square and in the area of the 10 Kursai well, and the minimum - in the area of the 13 Zap well. Akzhar.

The subsalt Upper Paleozoic sediments are the filling stratum, leveling the block structure of the lower part of the sedimentary cover. Paleo-uplift and faults limiting it are still well expressed in Carboniferous deposits, and in the subsalt

complex of the Lower Permian, by the time of Artinsky time, they have almost completely decayed.

In general, subsalt deposits on the Tamdykol ledge rise monoclinically from west to east, where the thickness of carbon deposits increases due to the appearance of carbonate strata KT- I , KT- II and terrigenous stratum TR- II in the section .

According to the results of 3D seismic surveys on Akzhar Vostochny Square, four main reflecting horizons are distinguished in subsalt deposits:

1) Horizon  $P_1$  (erosion surface - the roof of the Artin deposits - the sole of saline sediments of the kungur);

2) Horizon VIII ( $P_1'$ ) - the roof of the productive interval at the bottom of the Sakmara deposits;

3) Horizon  $P_2$ - presumably the roof of the Visean Carboniferous deposits;

4) Horizon  $P_3$ - erosion surface of terrigenous deposits of the Lower-Middle Devonian.

Horizons  $P_3$ ,  $P_2$  and VIII structurally repeat the foundation relief, have a common tectonic model. Horizon  $P_1$  is structurally a monoclinic surface complicated by low-amplitude folds of submeridional strike.

## 2.5 Oil and gas

The oil and gas potential of the North C Buzachi field is associated with Middle Jurassic and Lower Cretaceous deposits. The first industrial influx of oil from Neocomian deposits was obtained in 1975 in well G122, and from Jurassic deposits in well G130.

The data on the oil and gas potential of the North C Buzachi field are presented below in the variant of indexing productive formations from the 2008 report on reserves estimation.

Within the productive part of the field section, 8 productive strata are distinguished in Cretaceous deposits (A, A1, A2, B, C,  $G_B$ ,  $G_N$  and D1) and two (Yu-1 and Yu-2) in Jurassic. Oil and gas and oil deposits are confined to these strata. Neocomian formations A, A1 and A2 contain gas caps. Jurassic deposits contain the main reserves of the field.

The following is a brief description of productive horizons and associated deposits.

### **Plast A**

It is represented by cemented sands. It consists mainly of one, less often of two layers. The coefficient of dissection is 1.1, and the coefficient of sandiness is 0.315. In almost half of the wells, it is replaced by dense impermeable rocks, the distribution coefficient of the reservoir is 0.445.

The total thickness of the formation varies from 1.7 to 8.4 m, the effective gas-saturated power is from 0.6 to 3.0 m, the effective oil-saturated power is from 0.6 to 6.4 m.

The oil content of the reservoir according to the results of well testing was established in blocks II , V , VI , VII , IX and X. In block IX (well G170), gas was obtained during testing.

#### **Plast A1**

Stratum A1 is separated from overlying stratum A by a clay layer with a thickness of up to 2-3 m. It can be traced almost throughout the entire area of the field. The reservoir absence zones are mainly represented by small lenses, with the exception of the eastern part, where the reservoir absence zone occupies a significant territory, dividing block X into two parts . The distribution coefficient of the collectors is 0.768.

The segregation of the formation is low, in most wells it is a single formation, less often divided into several layers (up to five). The dissection coefficient is 1.5. Sandiness coefficient - 0.43.

The total thickness of the reservoir varies from 5.7 to 15.4 m, effective gas-saturated power - from 0.7 to 10.0 m, effective oil-saturated power - from 0.6 m to 10.6 m.

The productivity of the formation was identified in all blocks of the field, a gas cap was identified within the VI block.

#### **Plast A2**

It is represented by variegated siltstones of varying degrees of cementation. It consists mainly of 1-3 layers. The coefficient of dissection is 1.1, the coefficient of sandiness is 0.43. Formation A2 is sealed in more than half of the wells that have uncovered it. The distribution coefficient of the reservoir is 0.39. In the western part of the field it was discovered by single wells, in the east it is more widespread.

The total thickness of the A2 layer varies from 5.1 to 20.3 m, effective - from 0.6 to 10.1 m.

Plast A2 is productive only in the VI and X blocks of the field.

#### **Plast B**

Compared to the overlying A2 formation, B is slightly wider, but in many wells it is also replaced by impervious differences and its distribution is lenticular. The reservoir distribution coefficient is 0.39.

It consists of 1-3 interlayers, while the dissection coefficient is 1.4. The total thickness of formation B varies from 5.8 to 16.9 m, effective oil-saturated thickness - from 0.6 to 10.6 m. Sandiness coefficient is 0.30.

The oil content of the reservoir is established in IV , V , VI , VIa and X blocks.

#### **Plast B**

Formation B in lithological respect does not differ from the overlying strata, however, it has a much wider distribution over the area. Clay zones are located in the western and eastern parts of the deposit. The distribution coefficient of reservoirs throughout the reservoir is 0.86, and the sandiness coefficient is 0.31.

From 1 to 5 interlayers can be traced in the reservoir, the disaggregation coefficient is 1.8.

The total thickness of formation B varies from 9.8 to 27.1 m, and the effective oil-saturated thickness varies from 0.7 to 13.4 m.

The oil content of formation B is established in II , V , VI , VIa , VII , IX , X , XI, and XIV blocks of the field.

### **Plast G**

Plast G consists of three reservoir layers. The two upper ones can be traced practically over the entire area of the field, and the lower layer is lenticular in nature, the most extensive zones of its distribution are in blocks VI and X , in the rest of the territory the lower part of layer D is mossy. In this regard, when calculating reserves, stratum G was divided into two independent objects - upper (Gv) and lower (Gn).

### **Plast Guards**

The Gv layer among all Neocomian strata is the most consistent in area, the distribution coefficient of the reservoir is 0.95. It consists of several layers, the number of which varies from 1 to 9. The coefficient of formation stratification is 3.3. Another indicator of reservoir heterogeneity, the sandiness coefficient, is 0.24.

The total thickness of the formation varies from 10.7 to 40.5 m, the effective oil-saturated power - from 0.6 to 13.2 m.

The productivity of the Gv layer is established in VI , VI a, VII , IX , X, and XI blocks.

### **Plast Gn**

Collectors have local distribution, the most extensive zones of their development are in VI and X blocks. The distribution coefficient is 0.33. The total thickness of the reservoir varies from 6.2 to 38.9 m, effective oil-saturated thickness - from 0.6 to 7.5 m. The sandiness coefficient is 0.20. The stratum consists mainly of 1-3 interlayers, the stratification coefficient is 1.3.

The oil content of the reservoir is identified in the VI and X blocks.

### **Plast D1**

The D1 layer contains from 1 to 5 layers, although most often they are 2-3. The dissection coefficient is 1.3. The total thickness of the formation varies from 8.8 to 19.7 m, and the effective oil-saturated - from 0.6 to 9.1 m. The sandiness coefficient for the D1 formation is 0.22.

Productive reservoirs are identified in blocks VI , VIa , VII , IX , X , where oil deposits are associated with them. In block VIa, reservoir D1 consists of two layers, each of which contains an independent reservoir.

### **Yu-1 horizon**

It is represented by sand-siltstone rocks. The eastern part of the field is blurry. The horizon spread coefficient is 0.98.

It contains from 1 to 15 reservoir layers, the stratification coefficient is 4.8. Often the layers merge with each other, forming a single powerful reservoir.

The total thickness of the horizon varies from 3.3 to 89.6 m. A decrease in the thickness of the horizon is observed in the eastern direction, where it goes under the surface of the pre-Cretaceous erosion. Effective oil-saturated thickness varies from 6.2 to 59.9 m, gas-saturated - from 0.6 m to 13.4 m.

Horizon productivity has been proven by testing in 23 exploratory wells and numerous test results for production wells. The horizon is oil-bearing in II , III , IV , V , VI , VII , IX , X , XIV blocks, while the presence of a gas cap is established in the VI block. The gas cap was opened 35 production wells.

### **Yu-2 horizon**

It is represented by the alternation of siltstones, sandstones and clays. The horizon spread coefficient is 0.98.

It consists of several layers, the number of which varies from 1 to 10. The coefficient of formation stratification is 2.9. Another indicator of reservoir heterogeneity, the sandiness coefficient, is 0.44.

The total thickness of the horizon varies from 24.9 to 101 m. The effective oil-saturated thickness varies from 1.2 to 44.4 m.

The oil content of the horizon is set in blocks VI , X and XI .

Within the VI block, two domes (western and eastern) stand out, separated by a small deflection. Each of them is associated with an independent oil deposit. (Table B1)

### **3 Field seismic surveys and seismic data processing**

Field seismic surveys using the CDP-3 D method were carried out, as indicated above, in different years and in different areas ( *Central, Eastern and Western* ) and all of them always began with experimental work on the selection of conditions for the excitation of elastic vibrations, their registration and selection of a field system observations. Based on the analysis of these works, it was determined that for solving the geological task set by the Customer, the field observation systems presented in the tables for the Northern Buzachi area correspond to (Table C1).

Despite significant differences in field systems for surveys of different years, the quality of field seismograms is quite good, which, after appropriate alignment procedures, led to the acquisition of a combined cube of seismic information that allowed us to fulfill the geological tasks assigned to the reporting work.

The results of processing the obtained materials for the indicated field observation systems in the Computing Center of Paradyme Geophysical LLC showed that the applied 3D field observation systems for the North Buzachi structure are quite acceptable. And the obtained field seismic data for the considered territory are characterized mainly by good quality. Based on these data, it is possible to solve the set geological problems, both by structural interpretation and by identifying seismic wave field anomalies, possibly associated with hydrocarbon deposits (dynamic interpretation).

#### **3.1 Processing of seismic data in the time domain**

Basic 3D field seismic data processing.

- Data input.
- Description and assignment of geometry.
- Edition of tracks with 100% visual viewing and quality control geometry assignment.
- Analysis of input data (signal-to-noise ratio, amplitude-frequency characteristics, comparative definitions of the pulse shape and characteristics of the signal from various excitation sources: explosive and pulsed).
- Noise attenuation.
- Calculation and input of static corrections for topography and velocity inhomogeneities of the VChR based on refractive and tomographic operations. The level of reduction is (to be agreed upon), the reduction rate is determined by testing.
- Amplitude correction for spherical divergence.
- Muting the first intros.
- Surface-matched amplitude balancing.
- Surface-consistent predictive deconvolution.

- Sort data.
- Alignment of the amplitude spectrum.
- Band pass filtering.
- Preliminary speed analysis.
- Analysis and interactive correction of residual statics. (If necessary) \*
- Automatic correction of residual statics.
- Multiple Wave Suppression. (If necessary) \*
- Detailed interactive speed analysis on a 1.5km \* 1.5km grid.
- Repeated automatic static correction.
- DMO conversion.
- Entering kinematic corrections with the final speed law.
- Coherent filtering by non-cumulative data. (If necessary) \*

Time-variable bandpass filtering and amplitude adjustment.

## **3.2 Interpretation processing**

### **3.2.1 Migration before summation in the time domain**

Building a speed model.

- Testing methods and parameters (determining the maximum migration aperture).
- Migration of seismograms in the time domain using a velocity cube and subsequent correction of kinematic corrections and input of residual phase shifts.
- Summing migrated seismograms to produce a migrated total cube.

### **3.2.2 Migration before summation in the deep region**

Construction of a deep-speed model (DSM). It is performed by calculating the horizontal spectra of reservoir velocities, correlating them and aligning them over the area along the reference reflecting horizons determined by the total sections, and then recalculating the maps of times  $T_0(x; y)$  into depth maps using radiation migration.

- Depth migration before summing according to the full-wave algorithm with subsequent analysis of the residual kinematics from the deep migrated seismograms.
- Processing migrated seismograms before summing. This type of work includes:
  - Spectral balancing.
  - Coherent filtering to suppress random interference.
  - Time-variable bandpass filtering and amplitude adjustment.

The final stage of interpretation processing is considered to be the calibration of a deep cube from well information

### **3.2.3 The construction of the deep-speed model (DSM)**

The construction of DSM was carried out from a flat, intermediate, reduction level of 0 m .

To build the initial DSM, the summation speeds obtained during standard processing were used . The cube of the summing speed is transformed into the RMS speed, with subsequent conversion to the cube of interval speeds in the time domain . In order to control the quality of the obtained interval velocities, a migration in the time domain was performed prior to summing every tenth Inline according to the Kirchhoff algorithm.

### **3.2.4 Testing migration aperture parameters**

Using the obtained DSM, the migration aperture values were tested. Testing was performed using migration according to the Kirchhoff algorithm.

The aperture is the second migration parameter after the deep-speed model and depends on the magnitude of the expected drift of the seismic signal. The following apertures were tested for this area: 2000, 4000, 6000 and 8000 meters (Fig D 1-4). For migration, an aperture of 4000 m was chosen , since with this value a stable focusing of the images was achieved and a further increase in the length of the aperture did not bring an increase in information (Fig. D2).

### **3.2.5 Migration procedure and summation**

At the stage of depth migration of seismograms, the following actions were performed:

1. Depth migration before summation according to the CSFW algorithm.
2. Estimation of residual kinematics by migrated seismograms. The assessment was carried out automatically with a step of 125 m in Inline and 125 m in Crossline based on 3 points of CDP. The results of automatic picking over the entire cube were reviewed and adjusted manually. To construct a cube of residual kinematic corrections, smoothing in a window of 400 m \* 400 m was used .
3. The final summation of the deep migrated seismograms with the input of the residual kinematics and deep muting, obtaining the deep cube and recalculating it to the time scale (Fig. D5).

### **3.2.6 Post-migration processing**

At the final stage, the following procedures were performed for the efficient migrated cube:

- Spectral balancing (expansion of the amplitude spectrum),
- Time - variable band-pass frequency filtering,

- Coherent filtering to suppress random interference,
- Time - variable trace balancing.

Figure 6(Appendix D) shows the result of the depth migration of seismograms on a time scale after applying post-migration processing.

## **4 Interpretation of seismic materials**

Interpretation of geological and geophysical materials was carried out on the basis of productive materials obtained after their processing both in the time and in the deep regions.

The interpretation process itself was subdivided into two stages - structural and dynamic . Structural (based on deep migration) and dynamic (based on temporary migration) interpretation was carried out using the software of the company Paradigm .

### **4.1 Database for interpretation**

The database for the geological interpretation of the combined 3 D seismic cube consists of three main information blocks:

Regional geological information on the structure of the North-Buzachisk arch and the oil and gas potential of the Lower Cretaceous and Middle Jurassic sandstone strata within it.

Seismic data block - cubes after various processing options.

Well information.

### **4.2 Stratification of reflecting horizons**

In agreement with the Customer, in order to build a seismic-geological model, this report adopted the following system of indexing reflecting horizons and their confinement to the main structural-formation boundaries of the section (from bottom to top from pre-Jurassic formations to the apta inclusive). Indexation corresponds to the top of the interface between the lithologic-stratigraphic units or reservoir strata adopted for the region in the Texaco variant . The entire section is divided into five seismic stratigraphic complexes, and the obtained seismic-geological model of the structure is described by eleven reflecting horizons, among which reference and target ones stand out. In turn, by the method of correlation, the targets are divided into mappings according to the principle of phase correlation and conditionally allocated according to group correlation.

The following is the indexation and classification of reflecting horizons.

#### **I - Middle Jurassic seismic-geological complex:**

1. " V " - **Reference** reflecting horizon, confined to the roof of pre-Jurassic formations. It stands out everywhere in the wave field (positive phase) and quite confidently.

2. " **Top \_ Sand F** " (optional, roof Yu\_3) - the target reflecting horizon, confined to the roof of a strong long-lasting reflective pack, which generally

coincides with the end of the period of extensive coal deposition and the beginning of the most frequent marine offensives.

3. “ **Base \_ Delta** ” (near the top of the roof of the Yu-2 counting object) - the target reflecting horizon, confined to the roof of a clay pack that separates clay deposits of the transgression period - relative deep water from the sands of branched channels deposited during relative shallow water.

4. “ **Top \_ Delta** ” (the roof of the Yu1 counting object) - the target reflecting horizon, confined to the roof of the clay bundle that separates the clay deposits of the transgression period - relative deep water

5. “ **III** ” - **Jurassic-Cretaceous disagreement** ” - **Reference** reflecting horizon confined to the surface of the Pre-Ocomian erosion.

## **II - Lower Neocomian wedge-shaped seismic-geological complex:**

6. “ **Top \_ II - E** ” - near the top, the target reflecting horizon, confined to the roof of the reservoir in the Neocomian mass.

7. “ **Top II \_ D 3** ” - the target reflecting horizon, confined to the roof of the reservoir in the Neocomian mass.

8. “ **Top II \_ D 2** ” - the target reflecting horizon, confined to the roof of the reservoir in the Neocomian mass.

9. “ **Top II \_ D 1\_1** ” - the target reflecting horizon, confined to the roof of the reservoir in the Neocomian mass.

10. “ **Top II \_ D 1** ” - the target reflecting horizon, confined to the roof of the reservoir in the Neocomian mass.

11. “ **Reper D** ” - **Reference** reflecting horizon, confined to the roof of the reservoir in the Neocomian mass. He is “G”

## **III - Upper Neocomian subparallel seismic geological complex:**

12. “ **Top \_ II Gk** ” - the target reflecting horizon, confined to the roof of the reservoir in the Neocomian mass.

13. “ **Top \_ II Vk** ” - the target reflecting horizon, confined to the roof of the reservoir in the Neocomian mass.

14. “ **Top \_ II Bq** ” - the target reflecting horizon, confined to the roof of the reservoir in the Neocomian mass.

reflecting horizon, confined to the roof of the reservoir in the Neocomian mass.

15. “ **Top \_ II A2k** ” - the target reflecting horizon, confined to the roof of the reservoir in the Neocomian mass.

16. “ **Top Neo \_ A** ” - **Reference** reflecting horizon, confined to the roof of the reservoir in the Neocomian mass.

## **IV - Aptian seismic-geological complex:**

17. “ Top Apt \_ I ” - Reference reflecting horizon in apt.

18. “ Top Apt \_ II ” - Reference reflecting horizon in apt

### **4.3 Dynamic interpretation and attribute analysis**

A dynamic interpretation was made on the basis of temporary migration and was carried out using the software of the company Paradigm .

The basis for the dynamic interpretation of seismic data are the sedimentological models and facial maps obtained in the process of performing detailed sedimentological analysis.

#### **The main types of work performed in the framework of dynamic analysis:**

- Attribute analysis
- Seismic facies analysis
- Spectral decomposition
- AVO conversions
- Anisotropy prediction
- Inverse transforms (acoustic inversion, synchronous inversion)

The approach used to create geological models of the studied reservoirs allows to obtain a reliable result that provides the necessary information about the lateral and vertical variability of reservoirs, which serves as the basis for detailed three-dimensional modeling.

#### **4.3.1. Analysis of petrophysical properties of rocks for the problems of AVO analysis and amplitude inversion**

To establish a relationship between seismic attributes and calculation parameters, all available GIS material for the North Buzachi field was analyzed. For the tasks of dynamic interpretation, it is important to study the stiffness characteristics of the studied strata, which in the logging complex are represented by density and acoustic methods.

Before starting the analysis of the petrophysical properties, the production and geophysical curves transmitted by the Customer were prepared in a special way: an independent alignment of the logging material was made, in a number of wells an additive correction was made to the DT and RHOB curves . In addition, the RHOB , DT curves were smoothed with a step of 0.5 m vertically, and the intervals of high-amplitude emissions were corrected. As a result, a material suitable for the analysis of the petrophysical properties of the section was obtained.

### 4.3.2 Studying the stiffness properties of the target interval.

In the studied section, the reservoirs of terrigenous Lower Cretaceous and Middle Jurassic sediments are represented by weakly cemented sandstones (sands) and siltstones (siltstones) with a low content of clay material. The effective thickness of reservoirs of productive formations varies between 0.3–12.1 m for Neocomian rocks and from 0.3 to 28.4 m for Middle Jurassic rocks.

At the first stage, it was necessary to establish which of the stiffness parameters best solves the problem of dividing the section into a “collector” - “non-collector”. For this, histograms of the distribution of the values of DT velocity, RHOB density, and acoustic impedance AI were constructed.

The analysis of the dependences showed that there is a fairly close relationship only between bulk density and porosity (Fig. E2 (b)). So, for productive deposits of the studied area, the **density** is an informative parameter that allows you to evaluate the quality of the reservoir and distinguish the intervals of the reservoirs in the thickness. Therefore, in the next step, the porosity curves were converted into velocity curves (pseudo-velocity) using the Gardner equation. In addition, in order to convert the velocity cube into the cube of porosity, a dependence of the form  $Kp = f$  (pseudo-velocity) was constructed and the regression equation was calculated. The equation has the following form:

$$Kp = 0.54 - 0.0001 * Vp \quad (1)$$

In order to be able to calculate the lithology cube, pseudo-velocity histograms were constructed for three specific lithotypes (Fig. E4). These are sandstones, siltstones, as well as clays and compacted rocks. As expected, the separation by parameter is quite clear. It can be seen that reservoir rocks, represented by sandstones and siltstones, differ from clays and dense differences in lower velocity values. The level of pseudo-velocities of the latter exceeds 3550 m / s. Blocked reservoir differences (siltstones) are characterized by parameter values of 3350-3550 m / s, and sandstones <3350 m / s.

The analysis showed that the separation of gas-saturated reservoirs by the stiffness characteristics of the medium is possible only for non-clayey sandstones. However, according to the petrophysical characteristics, oil-saturated rocks cannot be separated from water-saturated reservoirs.

### 4.4 Attribute and seismic facies analysis.

A characteristic feature of attribute analysis is its versatility both in the choice of attributes themselves and in the spectrum of tasks for the solution of which it is applied.

Attribute analysis can be a study of both the dynamic characteristics of a seismic field and its derivatives, and the attributes obtained as a result of various transformations

The first group of attributes includes the formal parameters of the recording of the wave field: the amplitudes of the reflecting horizon, the frequencies calculated in different time windows, and their numerous derivatives, signal envelopes, etc.

The second group consists of attributes claiming physical meaningfulness, or a group of wave field transformants: acoustic and shear impedances calculated in inversion, AVO parameters and their derivatives, fluid factor, absorption, mixed cubes calculated by the method of spectral decomposition (RGB cubes), and etc.

**Attribute analysis** of seismic records involves the study of measurements of the kinematic and dynamic parameters of seismic waves - amplitudes, phases, frequencies - at a qualitative and quantitative level with the goal of their conversion into reservoir capacitance characteristics. At the first stage of attribute analysis, a qualitative assessment of the information content of seismic attributes is performed, for which both exploratory drilling data and data from previous reports, if any, are used. Further, in the presence of correlations between attributes and petrophysical characteristics, parametric maps are calculated.

**Seismic facies analysis** is an analysis of the geometric shape (configuration) of reflections, dynamic parameters of amplitudes, degree of frequency continuity, etc. There is no direct correlation between a certain type of wave pattern and lithological composition of rocks, however, analysis of the characteristics of reflections in combination with all available data, primarily with well logging data, allows us to make an assumption about sedimentation conditions and obtain acceptable lithology estimates.

Seismic facies analysis was performed in the software package « **Stratimagic** » using neural network technology (THC), which is based on the use of self-organizing neural network for recognizing and evaluating changes in the seismic waveform in the studied range. The result obtained is a sequence of color-coded model traces from which a map of seismic facies is formed, which reflects the distribution of heterogeneity of seismic data.

#### **4.5 Characterization of reservoirs according to the results of dynamic interpretation.**

According to the geological task, the analysis of the parameters of the target reservoirs was performed: **A + A1, A2, B, B, G, D0, D1, D2, D3, E** and **S (S0 + S1 + S2)** using the calculated cubes obtained as a result of AVO / AVA inversion, amplitude inversion and calculation of additional seismic attributes.

The studied productive strata are differently distinguished in seismic sections. Some of the strata form a wave reflection packet (**B, D, D, and S**), while others do not have an independent response and interfere with higher and lower strata (**A and A1**).

The analysis of petrophysical characteristics showed that the intervals of the reservoir of the studied section have low values of speed and density with respect to

the host rocks. Thus, reservoir layers in a seismic wave field are distinguished by a **negative phase** .

At the first stage, the distribution of amplitudes over a **cube of a partial angular sum of 5 ° –50 °** was analyzed . In general, maps of this parameter reflect the general distribution of amplitudes. At the same time, zones of lithological heterogeneity of the target layers, as well as elements of tectonic disturbances are clearly visible on them, and channel flows are confidently traced ..

A number of AVO attributes were calculated for the target layers, of which informative are: **Normal Incidence Reflectivity, Fluid Factor, Lambda \* Rho Reflectivity, Elastic Impedance Reflectivity** .

The **Normal Incidence Reflectivity** attribute carries information about both the saturation of the formation and its lithology. Therefore, it is advisable to additionally use other AVO attributes. One of these attributes is **Fluid Factor** , which displays the hydrocarbon saturation of various cut intervals and is suitable for predicting gas sands of any class. The **Lambda \* Rho Reflectivity** attribute is also a sensitive indicator of pore fluids , which characterizes the sensitivity of the rock skeleton to shear during the propagation of an acoustic wave in fluids. From the attribute **Elastic Impedance Reflectivity** it is possible to obtain information about the lithological structure of the studied interval. Note that all these attributes are a complex characteristic due to seismic and geological conditions, only to one degree or another reflecting the geological characteristics of the studied stratum. Despite this, obtaining areal distributions of various attributes for the formation allows a more complete dynamic interpretation and increases the reliability of establishing the zoning of the geological features of the studied formation.

As noted above, the collector is characterized by a negative phase in the roof of the collector. Thus, for layers **A + A1 , A2 , B, B , G** , group of layers **A** and layer **E** were obtained negative values AVO-distribution maps attributes that are presented in the following figures:

Normal Incidence Reflectivity - Formation **A2 , B, B , G** , group of layers **A** and layer **E** ; (example: Figure 4.49)

Fluid Factor -for layers **A + A1 , A2 , B, B , G** , group of layers **A** and layer **E** ; (example: Figure 4.68)

Lambda \* Rho Reflectivity -for layers **A + A1 , A2 , B, B , G** , group layers **A** and layer **E** ; (example figure 4.80)

Elastic Impedance Reflectivity - Formation **A + A1 , A2 , B, B , G** , group of layers **A** and layer **E**. (Example figure 4.94)

As already noted, the **minimum values of the pseudo-velocity** , if the reservoir is fully resolved, characterize the quality of the reservoir, and the **total temporary power** - its effective thickness.

Since **seismic facies analysis** allows us to evaluate the shape of the tracks and classify a given interval, establishing zoning due to differences in sedimentation conditions. It is clear that such an analysis is advisable only for formations that form a packet of reflections in a seismic wave field.

## CONCLUSION

In this diploma work, was considered the possibility of modern dynamic interpretation methods for studying Neocomia-Jurassic deposits. Based on the results of the work, the following conclusions and recommendations can be made:

Processing the combined cube of seismic information in the deep version, combined with drilling data for 693 wells, allowed us to create a skeleton model of the structure of the reporting area from the roof of the Pre-Jurassic complex to the roof of Aptian clays inclusive.

Dynamic processing of various options for temporary cubes based on interpretation data. The results of dynamic analysis, including work with coherence cubes, attribute analysis, allowed us to detail the structure of productive complexes of the Middle Jurassic and Neocomian.

A detailed comprehensive geological interpretation of all seismic and well information allowed us to create an updated seismological model of the structure of the North Buzachi field.

Based on this model, recommendations are given for optimizing production drilling and showing locations most suitable for appraisal drilling (western part of the area). Maps for productive formations, in addition, can be used to correct the layout of production and injection wells, to draw up plans for exploration and additional exploration of individual blocks and sections.

Separately, we should focus on recommendations for the laying of appraisal wells, the estimated depth of which should exceed 750 - 800 meters and open in the northern blocks of deposition of pre-Jurassic age. Opening these deposits will allow us to unequivocally answer the question about the prospects of the pre-Jurassic complex within the licensed territory.

## LIST OF REFERENCES

- 1 Fred J. Hilterman. Seismic Amplitude Interpretation. EAGE, 2001.
- 2 With astagna JP, Bazle ML., Kan TK Rock Phisics - The link between rock properties and AVO response. Offset - dependent reflectivity - Theory and practice of AVO analysis.-Soc.Expl.Geophys., 1993, pp135-171.
- 3 Voskresensky Yu.N. The study of changes in the amplitudes of seismic reflections for the search and exploration of hydrocarbon deposits. Moscow, 2001.
- 4 Zalyaev N.Z. "Technique for automated interpretation of geophysical well surveys". - Minsk, 1990.
- 5 Journal articles on the geology of the Buzachinsky arch.
- 6 Daukeev S. Zh., Votsalevsky E. S., V. M. Pilifosov et al. "The Deep Structure and Mineral Resources of Kazakhstan", Oil and Gas, Volume III, Almaty, 2002.
- 7 Popkov V. I. Tectonics of the pre-Jurassic sedimentary complex of the west of the Turan Plate // USSR Academy of Sciences. Geotectonics. Ed. The science. No. 4. 1986.

## Appendix A

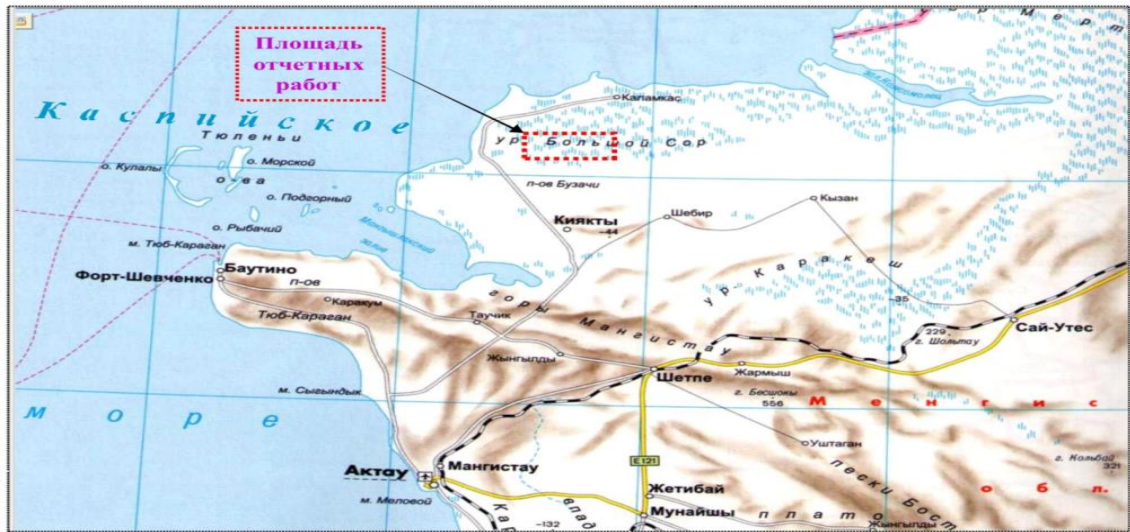


Figure 1 – Overview map of the North Buzachi field area

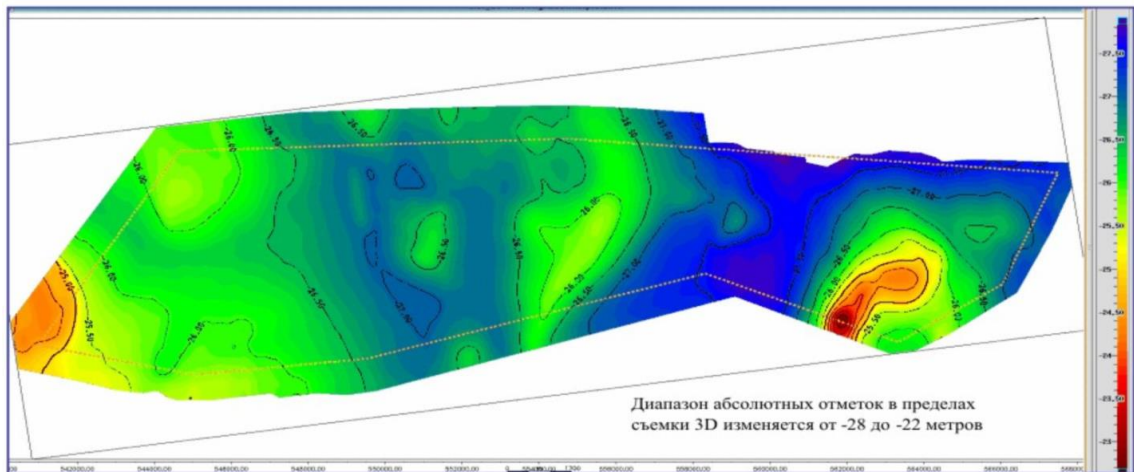


Figure 2 – Map of the relief of the work area

## Appendix B

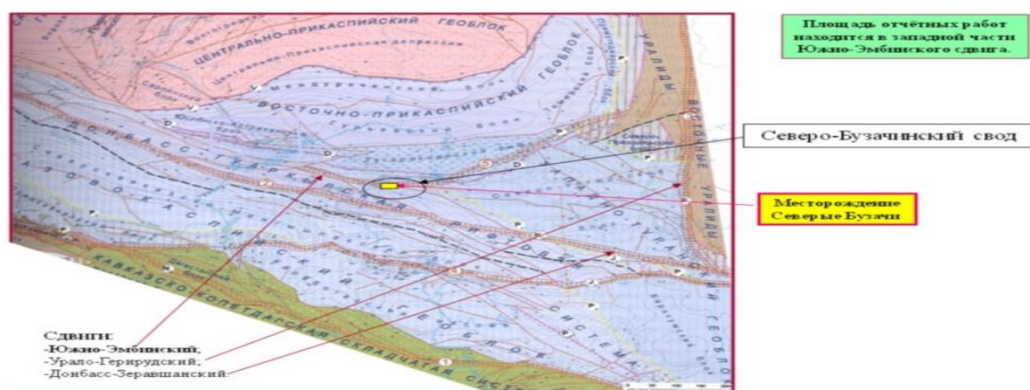


Figure 1 – Regional tectonic position of the research area (according to VolozhYu.A.

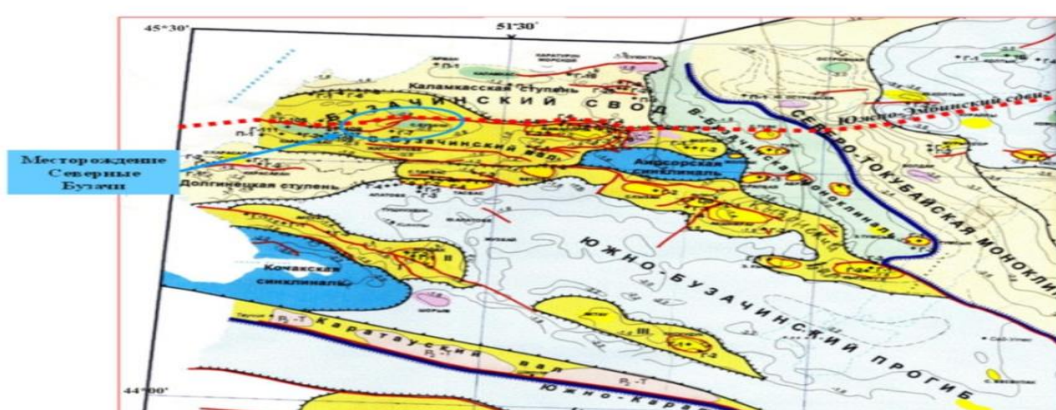


Figure 2 – Tectonic structure of the North-Buzachinsky arch

Table 1 – General physico-chemical properties of oil VIII productive horizon

Well, sampling interval	Density, kg/m <sup>3</sup>	Viscosity, cps		Content, %			Output gasol. before 200°C.
		20°C	50°C	paraffin	Sulfur	resin + asphaltenes	
Well 200 5036-5078m	813			2,6	0,07		34
Well 205 5038-5097m	812			н.о	0,5		31
Well 1 4995-5023m	873	24,9	24,98	0,34	0,12		26,8
Well G-1 5049-5074m	826	6,4	3,32		0,29	9,0	34
Well G-3, 5002-5032m	826	5,59	3,0	1,46	0,21	1,38	34

## Appendix C

Table 1 – Field work of 2008. Western part 37 km<sup>2</sup> (Azimut Energy Services JSC)

Description	Parameters
Full rated multiplicity	64
Bean Size (m * m)	12.5*12.5
Number of LP in strip	16
Number of RP on rep.line	64
Active Channels	1024
Step between RP on LP (m.)	25
Interval between LP (m)	100
Maximum value of minimum removals (m)	124
Maximum explosion- reception removal	1114
LP Location System	Pseudo cross
The step between the SP on the LP (m)	25
Number of shots per shooting area	16344
The number of wells in the group	4
Charge Weight (4x150)	600 g
Discretization step	2 ms.
Record length	3000 ms.

Inline numbers	1-544
Crossline Numbers	9-664

### Appendix D

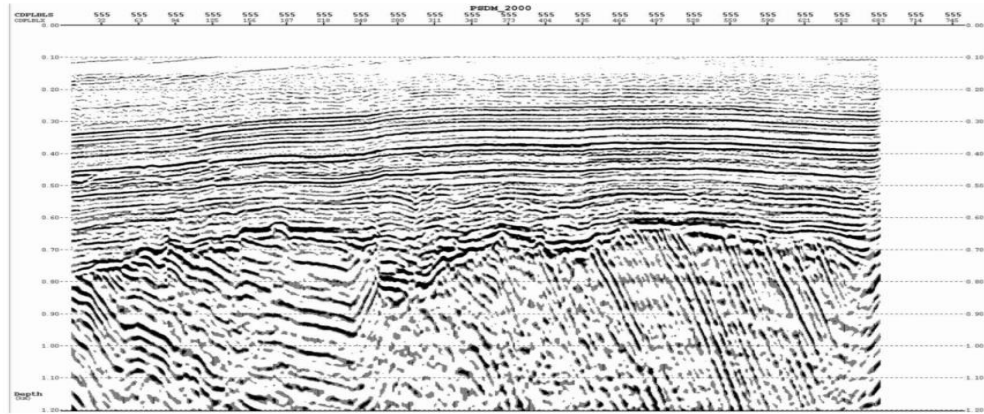


Figure 1 – Total section PSDM aperture 2000 m.

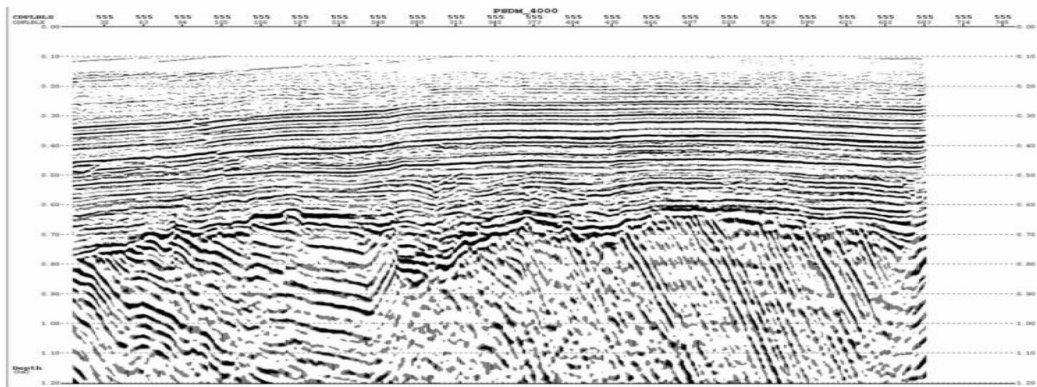


Figure 2 – Total section PSDM aperture 4000 m. Line 555

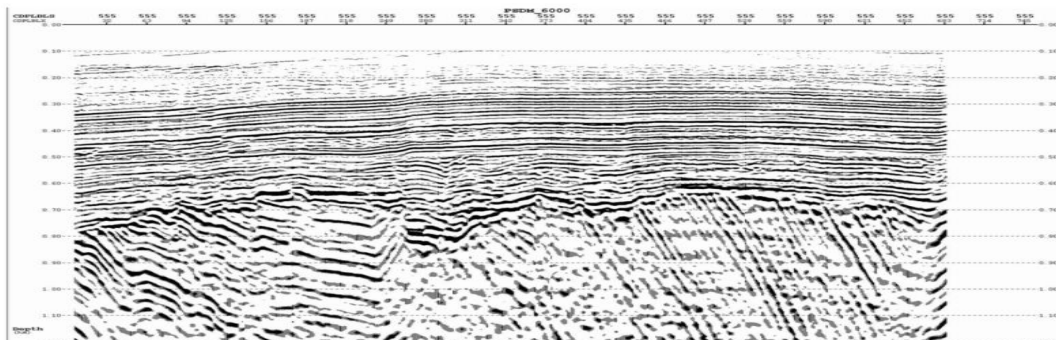


Figure 3 – Total section PSDM aperture 6000 м. Линия 555

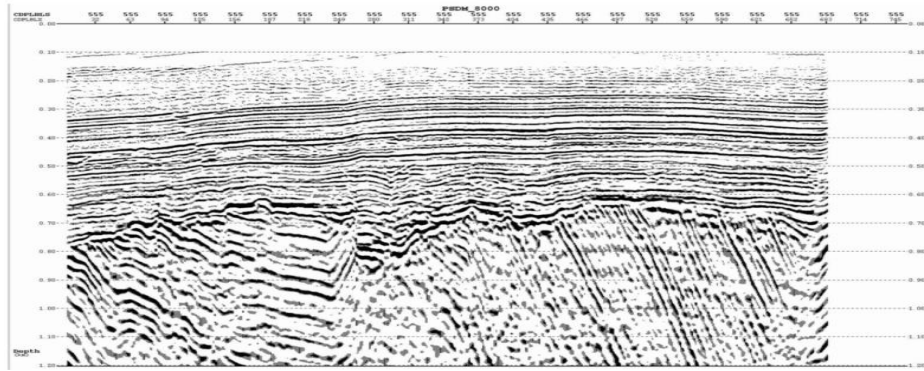


Figure 4 – Total section PSDM aperture 8000 m. Line 555

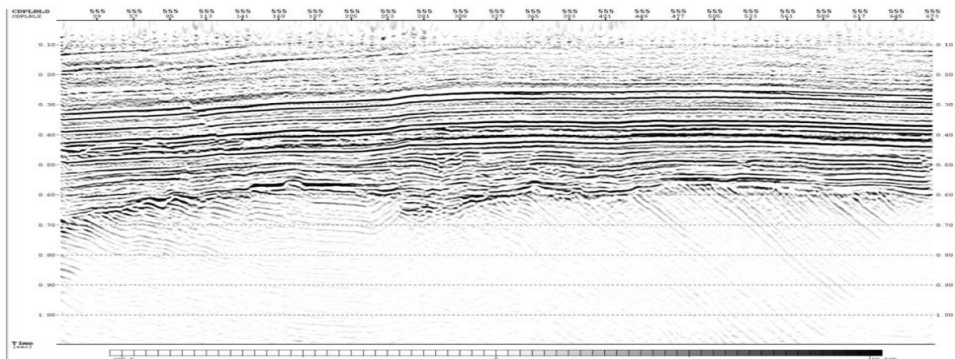


Figure 5 – Final total depth section recalculated to the time scale

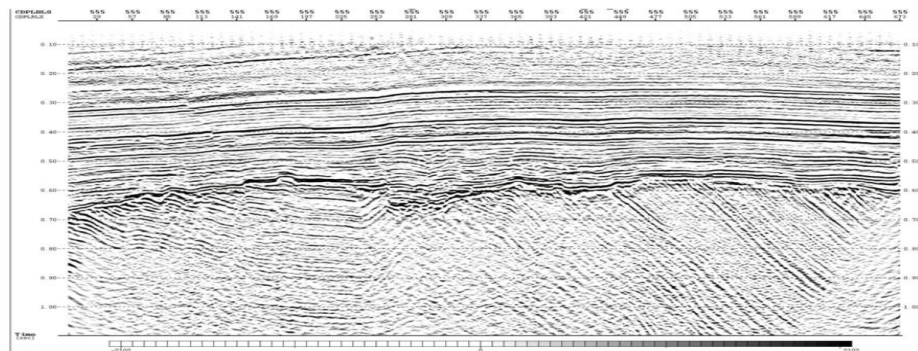


Figure 6 – The final total depth section, recalculated to the time scale with processing after summation. Line 555

## Appendix E

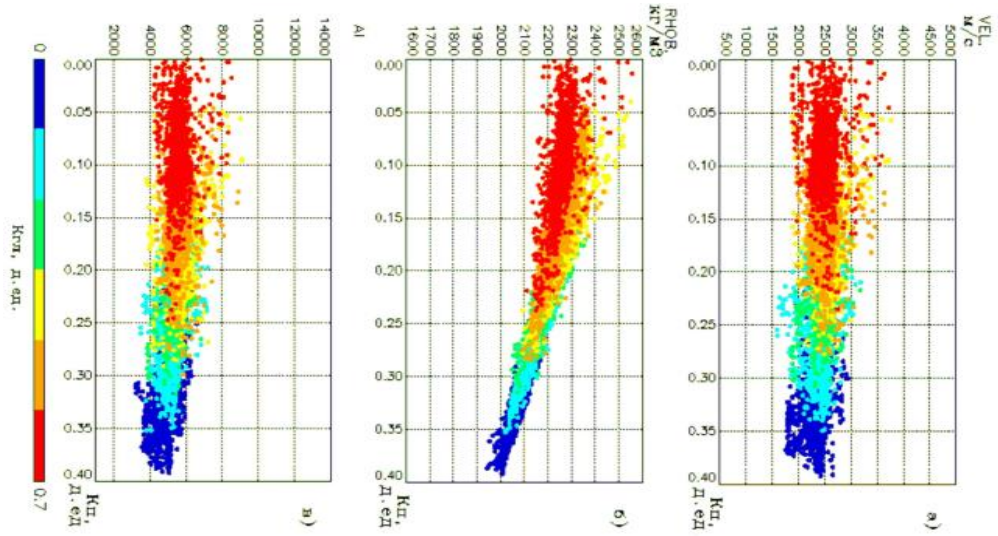


Figure 1 – Dependences of Vp, AI, DENSITY on porosity with color-coded clay.

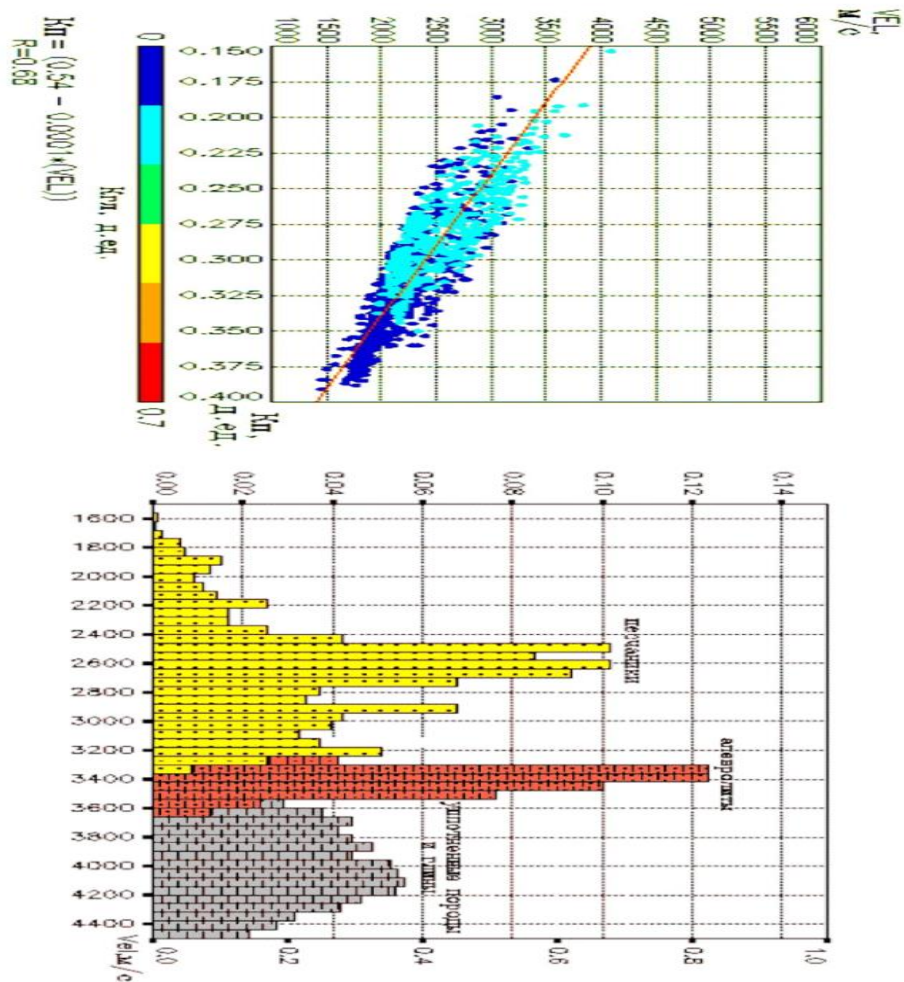


Figure 2-3 – The dependence of the pseudo-velocity on porosity with color-coded clay.

## Appendix F

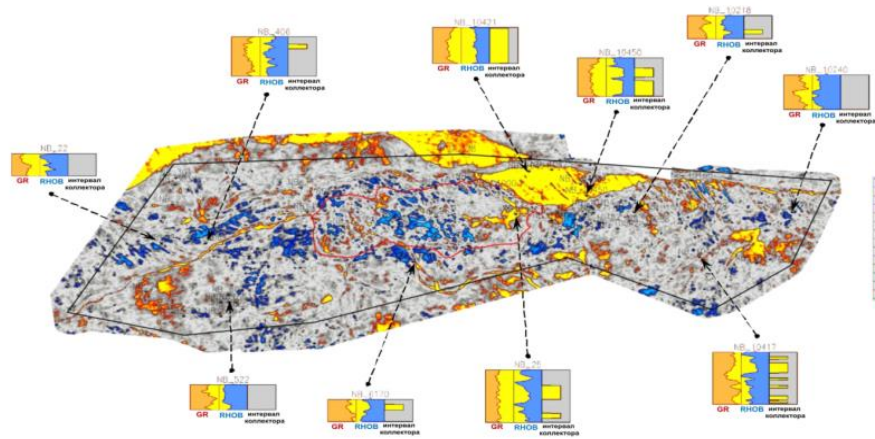


Figure 1 – Distribution of the amplitude of the Normal Incidence Reflectivity (R0) attribute over for Reservoir A2

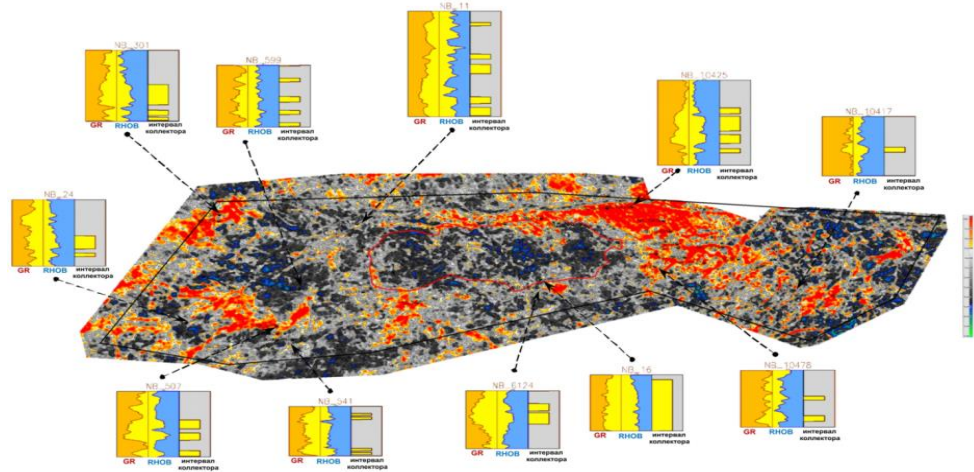


Figure 2 – Fluid Factor attribute amplitude distribution for reservoir B

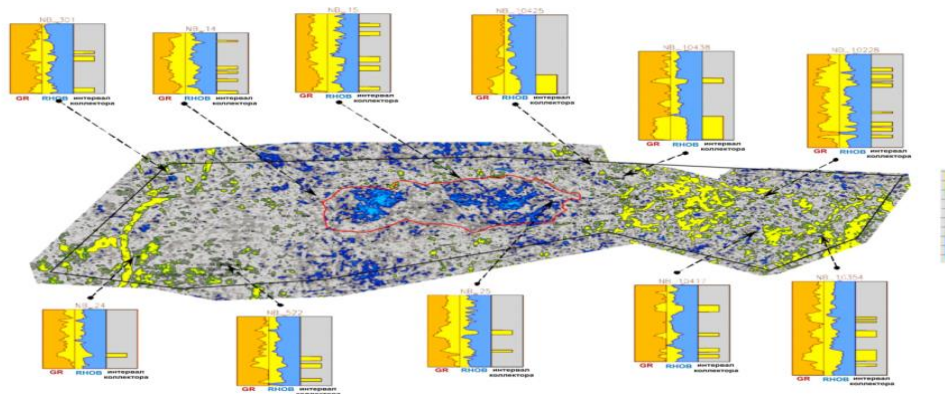


Figure 3 – The distribution of the amplitude of the attribute  $\Lambda * \text{Rho}$  Reflectivity in the reservoir G2

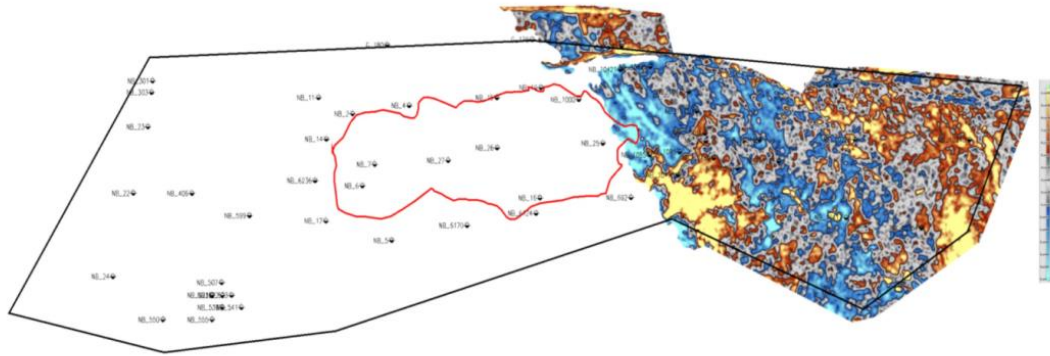


Figure 4 – Distribution of the amplitude of the Elastic Impedance Reflectivity attribute across the E formation